



April 2, 2009
NRC:09:023

Document Control Desk
U.S. Nuclear Regulatory Commission
Washington, D.C. 20555-0001

Response to Third Request for Additional Information Regarding ANP-10285P, "U.S. EPR Fuel Assembly Mechanical Design Topical Report"

Ref. 1: Letter, Ronnie L. Gardner (AREVA NP Inc.) to Document Control Desk (NRC), "Request for Review and Approval of ANP-10285P, 'U.S. EPR Fuel Assembly Mechanical Design Topical Report'," NRC:07:051, October 2, 2007.

Ref. 2: Letter, Getachew Tesfaye (NRC) to Ronnie L. Gardner (AREVA NP Inc.), "Third Request for Additional Information Regarding ANP-10285P, 'Fuel Assembly Mechanical Design Topical Report' (TAC No. MD7040)," January 15, 2009.

AREVA NP Inc. (AREVA NP) requested the NRC's review and approval of topical report ANP-10285P, "U.S. EPR Fuel Assembly Mechanical Design Topical Report" in Reference 1. The NRC provided a third Request for Additional Information (RAI) regarding this topical report in Reference 2. The response to the RAI is enclosed with this letter, ANP-10285Q4P, "Response to Third Request for Additional Information – ANP-10285P, 'U.S. EPR Fuel Assembly Mechanical Design Topical Report'."

The response to question 38 in ANP-10285Q4P impacts the fuel assembly liftoff margin analysis. The results of confirmatory analysis to demonstrate adequate fuel assembly liftoff margin will be provided to the NRC by April 30, 2009.

AREVA NP considers some of the material contained in the attachments to this letter to be proprietary. As required by 10 CFR 2.390(b), an affidavit is enclosed to support the withholding of the information from public disclosure. Proprietary and non-proprietary versions of the response are attached.

If you have any questions related to this submittal, please contact Ms. Sandra M. Sloan, Regulatory Affairs Manager for New Plants. She may be reached by telephone at 434-832-2369 or by e-mail at sandra.sloan@areva.com.

Sincerely,

Ronnie L. Gardner, Manager
Corporate Regulatory Affairs
AREVA NP Inc.

Enclosures

cc: G. Tesfaye
Docket No. 52-020

D077
NRO

AREVA NP INC.

An AREVA and Siemens company.

requested qualifies under 10 CFR 2.390(a)(4) "Trade secrets and commercial or financial information."

6. The following criteria are customarily applied by AREVA NP to determine whether information should be classified as proprietary:

- (a) The information reveals details of AREVA NP's research and development plans and programs or their results.
- (b) Use of the information by a competitor would permit the competitor to significantly reduce its expenditures, in time or resources, to design, produce, or market a similar product or service.
- (c) The information includes test data or analytical techniques concerning a process, methodology, or component, the application of which results in a competitive advantage for AREVA NP.
- (d) The information reveals certain distinguishing aspects of a process, methodology, or component, the exclusive use of which provides a competitive advantage for AREVA NP in product optimization or marketability.
- (e) The information is vital to a competitive advantage held by AREVA NP, would be helpful to competitors to AREVA NP, and would likely cause substantial harm to the competitive position of AREVA NP.

The information in the Document is considered proprietary for the reasons set forth in paragraphs 6(b) and 6(c) above.

7. In accordance with AREVA NP's policies governing the protection and control of information, proprietary information contained in this Document have been made available, on a limited basis, to others outside AREVA NP only as required and under suitable agreement providing for nondisclosure and limited use of the information.

8. AREVA NP policy requires that proprietary information be kept in a secured file or area and distributed on a need-to-know basis.

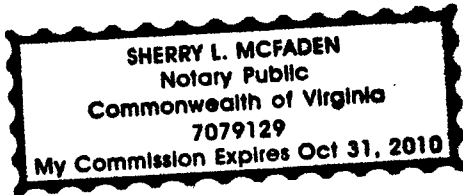
9. The foregoing statements are true and correct to the best of my knowledge,
information, and belief.



SUBSCRIBED before me this 27th
day of March 2009.



Sherry L. McFaden
NOTARY PUBLIC, COMMONWEALTH OF VIRGINIA
MY COMMISSION EXPIRES: 10/31/10
Reg. # 7079129



Response to Third Request for Additional Information—ANP-10285P
“U.S. EPR Fuel Assembly Mechanical Design Topical Report”
(TAC NO. MD7040)

- RAI-31.** *The following questions are related to a concern with the use of the RODEX2-2A code for SBLOCA analyses, particularly at burnup levels greater than 10 GWd/MTU. Because the code does not have a burnup dependent fuel thermal conductivity model, the code may under-predict fuel stored energy and fuel temperatures, and over-predict fuel thermal conductivity. The fuel temperature data used to verify this code above 10 GWd/MTU was very limited and based on measurements from only three rods that are not prototypical of current PWR fuel designs, including EPR. Also, the NRC confirmatory calculations with the FRAPCON code have been completed as per the input and output as calculated by S-RELAP5 provided in RAI-29 for SBLOCA. The confirmatory calculations demonstrated that the fuel centerline temperature is over 350°F higher than that calculated with the RODEX2-2A code at a peak LHGR of 13.4 kW/ft near the end of cycle 1.*
- a. *What is the difference between the RODEX2 code approved by NRC 25 years ago and the RODEX2-2A code being used for SBLOCA as discussed in response to RAI-29?*
 - b. *An example calculation is needed on the impacts of higher fuel stored energy, for example 350°F higher fuel centerline temperature, and lower fuel thermal conductivity due to degradation with burnup at moderate to high burnup levels on SBLOCA peak cladding temperatures.*
 - c. *Because this may be impacted by a burnup dependence on fuel thermal conductivity, what is the process used to select the burnup level at which the SBLOCA analyses are performed?*
 - d. *Is the RODEX2-2A code or its models used for determining fuel temperatures for other analyses besides SBLOCA?*

Response to RAI-31:

- a. The results of analyses are the same for the RODEX2 code and the RODEX2-2A code. The RODEX2A code was created for boiling water reactor (BWR) analyses and was approved by the NRC. The RODEX2-2A code is the combination of RODEX2 and RODEX2A into a single code version. The NRC-approved models for RODEX2 or RODEX2A are chosen through input. The NRC was informed of the consolidation of these two codes into a single code version in the letter NRC:01:025 dated September 10, 2001.
- b. The impact of stored energy on small break loss of coolant accident (SBLOCA) is addressed in the Response to U.S. EPR FSAR RAI 167, Question 15.06.05-39 and Question 15.06.05-42.
- c. The most significant burnup dependent effect on SBLOCA is the axial shape. A top peaked shape with the peak linear heat generation rate (LHGR) closest to the top of the fuel region is the most conservative axial shape. This shape occurs at end-of-cycle (EOC) and thus an EOC burnup is chosen for the SBLOCA analyses. Decay heat also has a significant impact on SBLOCA, and a fuel rod in its first cycle of operation is also

chosen because this fuel rod will have the highest power and the highest decay heat.

- d. The RODEX2-2A code is only used for SBLOCA analyses for the U.S. EPR.

- RAI-32.** *The original approval for RODEX3 was limited to applications below a burnup of 10 GWd/MTU, however the application provided for LBLOCA is above this burnup level. The concern with the use of the RODEX3A code is that the code does not have a burnup dependent fuel thermal conductivity model, therefore it may under-predict fuel stored energy and over-predict fuel thermal conductivity for LBLOCA analyses, particularly at burnup levels greater than 10 GWd/MTU.*
- a. *What is the difference between the RODEX3 code approved by NRC 13 years ago in ANF-90-145P Volumes 1 and 2 and the RODEX3A code being used for initializing LBLOCA as discussed in RAI-29? Provide the reference for the NRC approval of RODEX3A.*
 - b. *The correction for RODEX3A biased prediction of fuel centerline temperatures as stated in Section 4.3.3.2.1 of EMF-2103 is negative, or decreasing the predicted fuel temperatures, as a function of burnup. This appears to be incorrect, because this should be a positive addition to fuel centerline temperature. If this interpretation is correct, the positive addition in EMF-2103 to fuel centerline temperature appears to be much smaller than the percent per 10 GWd/MTU under-prediction in fuel centerline temperature recommended in the 1995 technical evaluation report (TER) of RODEX3. In addition, the degradation in fuel centerline temperature near peak LOCA conditions based on Halden data and several other recent fuel performance codes including the Halden, FRAPCON-3.3, and a recently approved AREVA fuel performance code RODEX4, results in approximately a 3.4 percent increase in fuel centerline temperature per 10 GWd/MTU starting from zero burnup levels at constant power and gap conductance. This degradation is also significantly greater than the correction provided in EMF-2013.*
 - c. *No S-RELAP5 predictions of initial conditions for RLBLOCA were found in the response to RAI-29 as requested, such as predicted centerline and volume average fuel temperatures, gap conductance, and rod pressures at the LHGR limits. Provide the initial centerline and volume average fuel temperature calculated with the S-RELAP5 code for the hot rod at the hot axial node along with rod pressure and gap conductance at the limiting burnup level, such that a comparison can be made to those calculated with the NRC code. This will help address the concern in question 31.b above on whether the RODEX3A code under-predicts fuel temperature.*
 - d. *Because it will be impacted by a burnup dependence on fuel thermal conductivity, what is the process used to select the burnup level at which the LBLOCA analyses are performed? Why is there a difference in burnup level at which RLBLOCA and SBLOCA are evaluated at 21 GWd/MTU and 32 GWd/MTU rod average, respectively? The power decrease with burnup due to depletion should be the same for the same core, and power should be the main driver for limiting conditions for both events.*
 - e. *Provide the peak LHGR limit versus fuel burnup for the EPR core based on the depletion calculation.*

- f. Is the RODEX3A code or its models used for determining fuel temperatures for other analyses besides LBLOCA?*

Response to RAI-32:

- a. The NRC approved the RODEX3A code in the realistic large break loss of coolant accident (RLBLOCA) analyses in EMF-2103PA, Revision 0 dated April 2003. EMF-2103PA, Revision 0 discusses the RODEX3A code in Sections 3.4, 3.4.1, and 4.3. Concerning the relationship between RODEX3 and RODEX3A, EMF-2103PA, Revision 0 states:

“RODEX3 (Reference 6) has been approved for use in providing input to the RLBLOCA analyses under certain conditions. These conditions have been addressed in the methodology and are discussed in Section 4.3. Following approval of RODEX3, the code was modified to provide the required input to the S-RELAP5 code. At that time the code was renamed RODEX3A (References 7 and 8). The RODEX3A code provides equivalent results on all benchmarks used for the approved RODEX3 code.”

Reference 6 refers to the RODEX3 topical report, ANP-90-145PA, dated April 1996, Reference 7 refers to the theory manual for RODEX3A, EMF-1557P, and Reference 8 refers to the RODEX3A code verification and validation manual. A copy of References 6 and 7 were provided to the NRC, along with other supporting documents, in the letter NRC:01:037, James F. Mallay (AREVA NP) to Mr. Kalyanam (NRC), “NRC Review of EMF-2103(P) Revision 0, Realistic Large Break LOCA Methodology for Pressurized Water Reactors,” dated August 21, 2001. EMF-2103PA, Section 4.3 discusses stored energy, specifically in Section 4.3.3.2.1. A more detailed analysis of the information in EMF-2103PA, Section 4.3.3.2.1 is provided in EMF-2102P, which was also provided to the NRC with the letter NRC:01:037.

The differences between the version of RODEX3A used in the RLBLOCA topical report, EMF-2103PA, and RODEX3 used in the topical report ANP-90-145PA are discussed in EMF-2102P, Section 5.8. The differences in the regression coefficient and standard deviation as compared to the benchmark data set are small and are attributed to minor codes changes over the years as a result of errors identified in code verification activities and due to computer platform changes.

- b. The correction to the centerline temperature calculation is expressed as a negative value and is subtracted from the RODEX3A calculated value. The result is an increase in the centerline temperature. The comparison of RODEX3A to benchmark data and a discussion of its conservatism with respect to centerline fuel temperature are presented in the Response to RAI-45.
- c. The RLBLOCA methodology is a statistical method that treats time in cycle, and thus burnup, as a statistical parameter. The analyses are performed for a range of burnup rather than at a limiting burnup. The response to U.S. EPR FSAR RAI 167, Question 15.06.05-38 provides the initial condition information. The conservatism in the centerline temperature calculation is discussed in the Response to RAI-45.
- d. The LBLOCA is analyzed with a statistical methodology that treats burnup as a statistical parameter, while the SBLOCA is analyzed with a deterministic methodology that uses a

burnup associated with a conservative statepoint. A comparison of the burnup where SBLOCA is performed with the burnup associated with the RLBLOCA case with the highest PCT is not meaningful.

- e. The peak linear heat generation rate (LHGR) limit for the U.S. EPR is constant.

Figure 32-1: U.S. EPR Core Peak LHGR versus Pin Exposure depicts the U.S. EPR core peak LHGR versus pin exposure for a core with four batches of fuel based on the depletion calculation. Fresh, once-burnt, twice-burnt, and thrice-burnt assemblies are represented in the figure. The peak LHGR for the cycle occurs in the fresh fuel. In general, the peak LHGR shows a downward trend with additional cycle time. As assemblies are burned in additional cycles, the batch peak LHGR shows a decreasing trend. The LHGR data presented in Figure 32-1 includes uncertainties.

Figure 32-1: U.S. EPR Core Peak LHGR versus Pin Exposure



- f. The RODEX3A code is not used for determining fuel temperatures for any analyses other than LBLOCA.

RAI-33. *The proposed bounding history methodology discussed in response to RAI-21 appears to be reasonably conservative, as long as the same identical core loading or less aggressive loadings at moderate to high burnup are used for all future core reloads. For example, the bounding history will change with different fuel management patterns and these future patterns may have a higher bounding history. The current methodology requires that if the planned power history, based on calculations of expected fuel operation, exceeds the bounding history, then the planned history will be used for the rod pressure analysis. Of concern is whether this approach of using planned power histories will become the norm, rather than a bounding history for the rod pressure analysis, because planned histories do not account for calculational uncertainties and possible uncertainties due to differences between planned and actual operating histories. For example, the bounding history will become less conservative if future cores and reloads have multiple rods that exceed this bounding history, or if plant power upgrades are introduced. In order to address this concern, discuss when a new bounding power history would be developed based on new depletion calculations for a given fuel management. This applies when more than one rod from a fuel batch or core exceeds the previously assumed bounding history or when the level of conservatism, between bounding and calculated, is reduced by a given amount.*

Response to RAI-33:

The concern about the use of planned power histories is based on the assumption that no uncertainties are accounted for when a planned power history is used with or in place of the bounding power histories, which is incorrect. The NRC-approved methodology requires that the planned power history linear heat generation rate (LHGR) be increased to account for power history uncertainty. The primary use of a planned power history is that for a specific cycle, a planned power history is more conservative for some exposure period than the bounding power histories that have been used previously.

There are situations, including variations in fuel rod enrichments, gadolinia concentrations, cycle length, or a significant change in the loading pattern, when a revised bounding power history may be developed based on new cycle calculations..

The power histories used in the analyses for the ANP-10285P topical report are based on determining, [

]. An example for a UO₂ rod with no gadolinia is shown in Figure 33-1: 18-Month Equilibrium Cycle Maximum LHGR Power Histories for UO₂ Fuel Rods. Each type of fuel rod loaded in the core (each type is defined by the enrichment and gadolinia loading) is examined in the neutronics core designs to determine the maximum LHGR at each depletion step. In Figure 33-1, there are three fuel rods with an enrichment of 4.8 w/o U235 and two with an enrichment of 4.3 w/o U235. [

]. The effect of anticipated operational occurrences (AOO) is included in the analysis to determine the maximum fuel rod internal pressure. For example, for the UO₂ fuel rods in an 18-month cycle design, [

]. This approach is explicitly considered as part of the approved methodology in the COPERNIC topical report, BAW-10231PA Revision 1, Section 12.1.1, (Reference 17 of ANP-10285P). The method provides the option to analyze [

].

Figure 33-1: 18-Month Equilibrium Cycle Maximum LHGR Power Histories for UO₂ Fuel Rods



RAI-34. *The original RAI-21 requested the applicant to “identify those transients that are bounding for the Condition 1 and 2 events in terms of fission gas release and rod pressure.” The limiting transients were not identified as requested. Identification of the limiting Condition 2 transient is of particular interest to determine if the assumed time at power for this event is appropriate, and to evaluate whether other Condition 2 events may be more bounding in terms of fission gas release.*

Response to RAI-34:

The transients (anticipated operational occurrences (AOO)) that are potentially bounding for fission gas release are characterized as an increase in heat removal by the secondary system and as a reactivity and power distribution anomaly. The transients considered are as follows:

U.S. EPR FSAR Tier 2, Section 15.1: Increase in Heat Removal by Secondary

- Decrease in feedwater temperature.
- Increase in feedwater flow.
- Increase in steam flow.
- Inadvertent opening of steam generator (SG) relief or safety valve.

U.S. EPR FSAR Tier 2, Section 15.4: Reactivity and Power Distribution Anomaly

- Uncontrolled rod cluster control assembly (RCCA) withdrawal from subcritical or low power startup condition.
- Uncontrolled RCCA withdrawal at power.
- Single RCCA withdrawal.
- RCCA misalignment.
- RCCA drop.
- Startup of the reactor coolant pump (RCP) in inactive loop.
- Inadvertent decrease in boron concentration in the reactor coolant system (RCS).
- Inadvertent loading and operation of fuel assembly in improper position.

The increase in the linear heat generation rate (LHGR) of the fuel rod and the duration of the power ramp in the fuel performance code COPERNIC calculations simulating the bounding fission gas release transient are selected to bound these characteristics for the potential transients.

The analyses of the transients demonstrate that the transients terminated in less than four minutes, which is less than the [] time at an increased LHGR required for the COPERNIC analyses by the NRC-approved methodology. The analyses of the transient power excursions show that they had core power excursions less than the [] percent for Condition I transients and [] percent for Condition II transients used in the COPERNIC fuel rod internal gas pressure analyses.

RAI-35. *Provide the best estimate, without fabrication or code and model uncertainties, of rod pressure prediction using the bounding power history and transients provided in RAI-21. The fuel average temperature provided in Figure 5-6 of the topical report appears to be the average temperature, averaged radially and axially over the rod. Also, provide the peak axial centerline temperature and peak axial node fuel average temperature, radially averaged as a function of rod average burnup, for this calculation.*

Response to RAI-35:

The results for the best-estimate rod internal gas pressure using the bounding power history, but without the fabrication or code and manufacturing uncertainties for the UO₂ fuel rod in the 18-month equilibrium cycle, is provided in Figure 35-1: UO₂ Fuel Rod Internal Pressures for 18 Month Equilibrium Cycle. Figure 35-1 also includes the bounding rod internal pressure presented in ANP-10285P, Figure 5-7, which shows that the maximum bounding pressure is [] psia. The best-estimate rod internal gas pressure using the same bounding power history with simulated transients is [] psia.

Figure 35-1: UO₂ Fuel Rod Internal Pressures for 18 Month Equilibrium Cycle

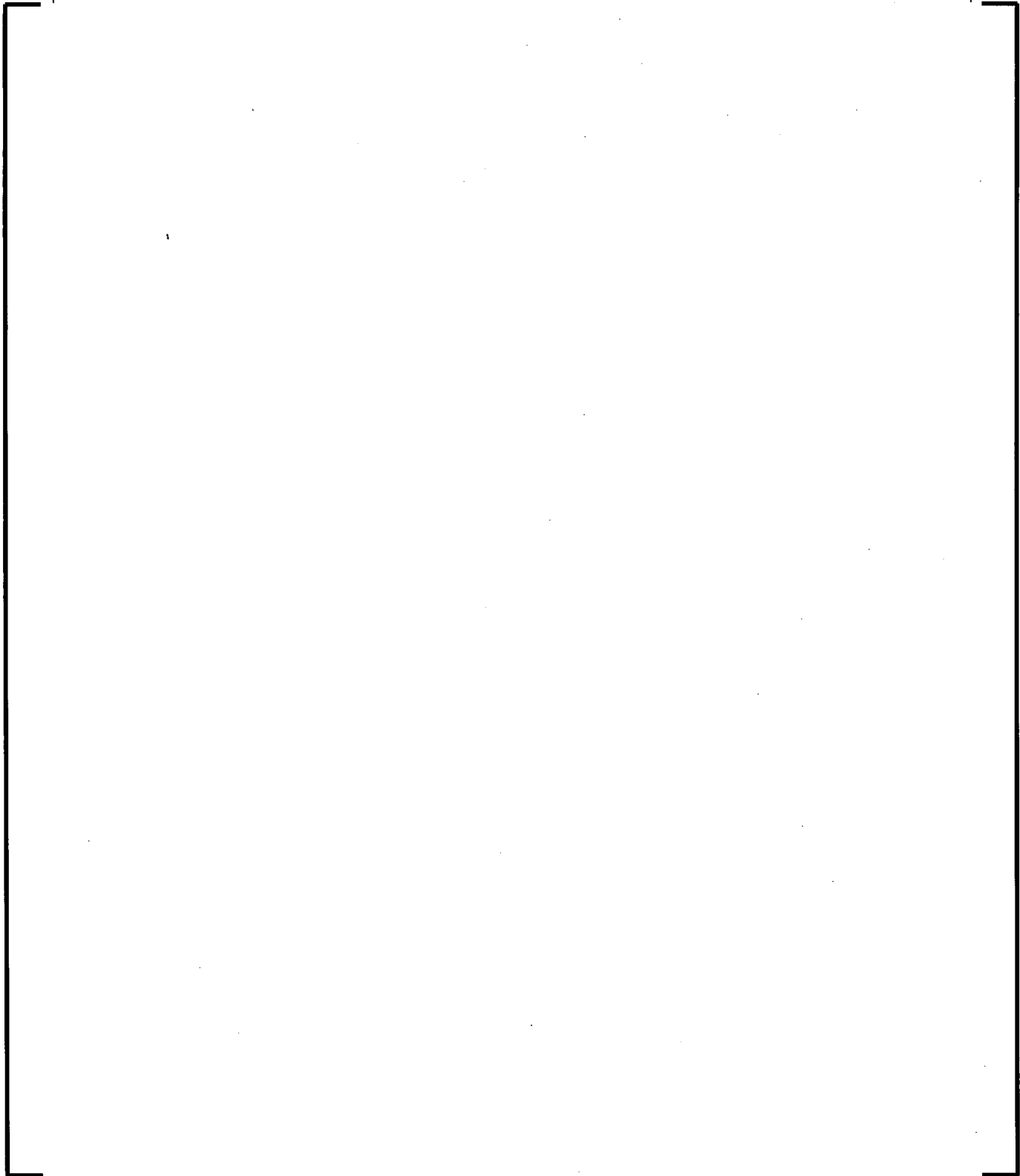


The centerline and radially-averaged fuel temperatures are obtained for axial elevations from the calculations using the bounding power history with the simulated transients. At each burnup step, the maximum value of the axial elevations is then compiled into a single set of data for the maximum centerline and maximum average temperature as a function of fuel rod average burnup. The locations of the maximum values vary axially as a function of the location of the maximum linear heat generation rate (LHGR) and the local thermal property conditions. The maximum temperatures for the radially-averaged and peak centerline temperatures are provided in Figure 35-2: UO₂ Fuel Rod Maximum Centerline and Radially Averaged Temperatures for 18-Month Equilibrium Cycle. Figure 35-2 also shows the fuel rod axially averaged fuel temperatures from ANP-10285P, Figure 5-6. Table 35-1: Values for the UO₂ Fuel Rod Pressure and Temperature RAI-35 Figures provides the pressure and temperature data used in the figures.

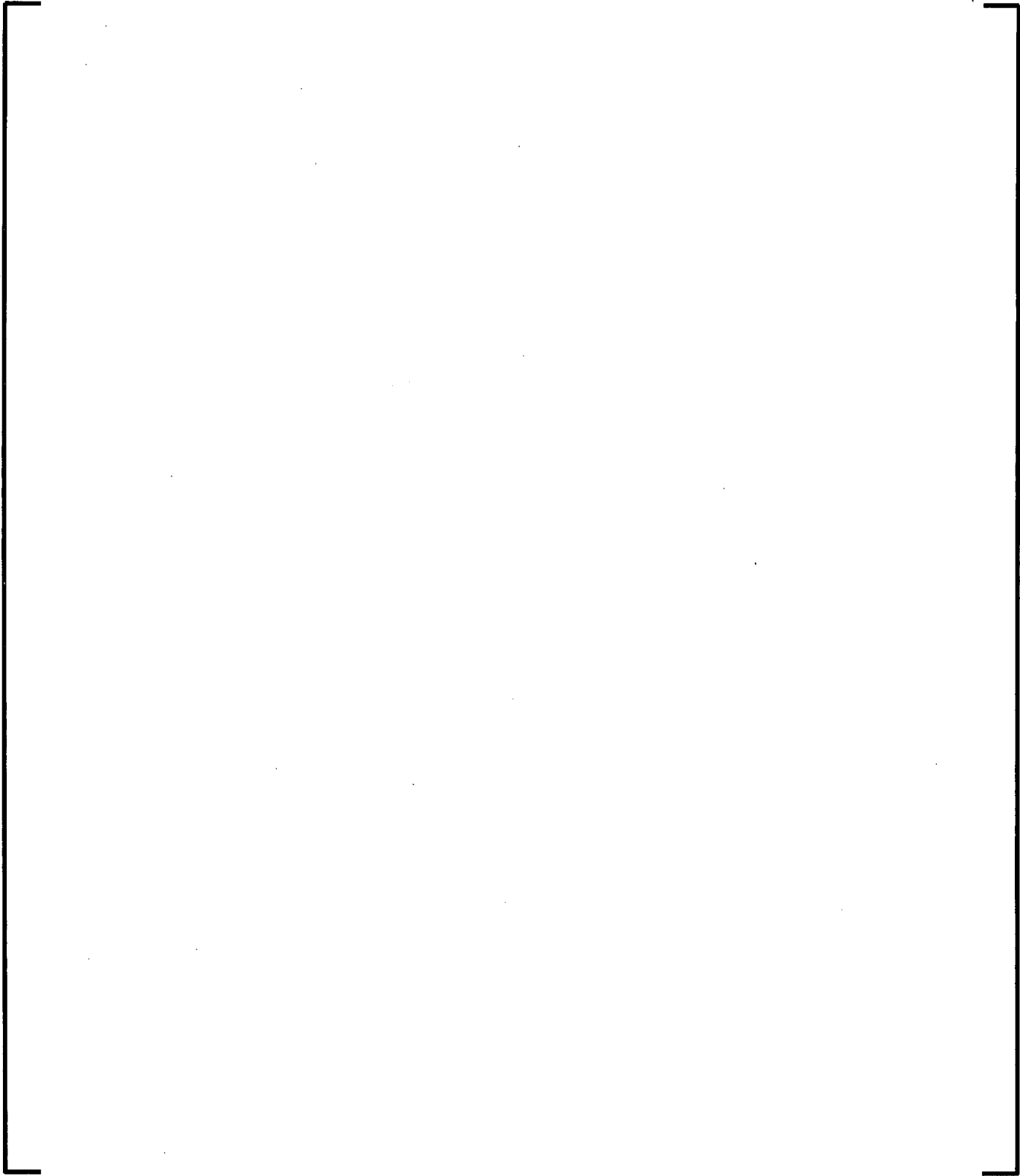
Figure 35-2: UO₂ Fuel Rod Maximum Centerline and Radially Averaged Temperatures for 18-Month Equilibrium Cycle



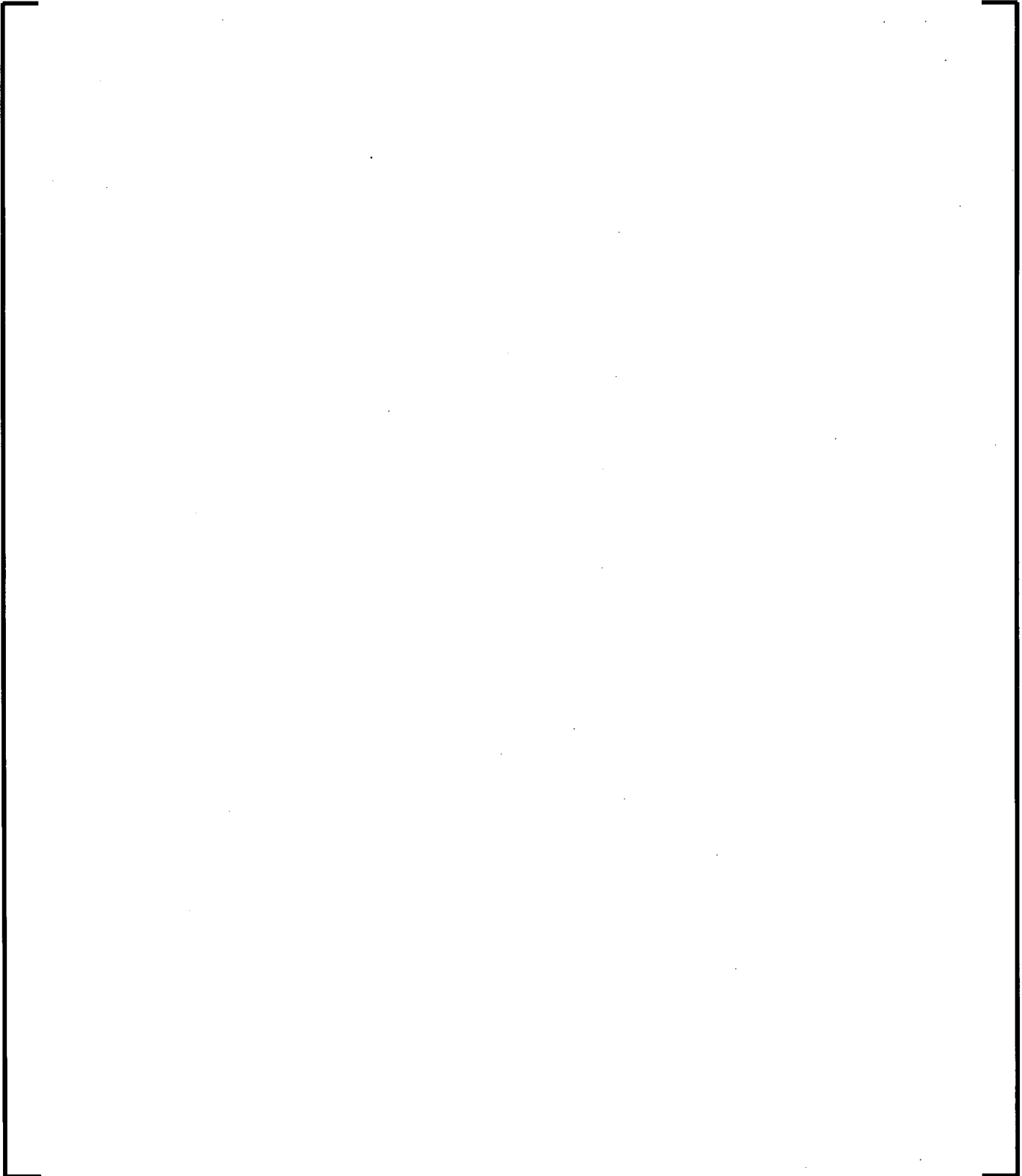
**Table 35-1: Values for the UO₂ Fuel Rod Pressure and Temperature RAI-35 Figures
(3 Sheets)**

A large, empty rectangular frame with a thick black border, intended for the table content. The frame is currently blank.

**Table 35-1: Values for the UO₂ Fuel Rod Pressure and Temperature RAI-35 Figures
(3 Sheets)**

A large, empty rectangular frame with a thin black border, occupying most of the page below the caption. It is intended to contain the data for Table 35-1, which is split across three sheets.

**Table 35-1: Values for the UO₂ Fuel Rod Pressure and Temperature RAI-35 Figures
(3 Sheets)**

A large, empty rectangular frame with a thin black border, occupying most of the page below the caption. It is intended for the data from Table 35-1, which is spread across three sheets.

RAI-36. *The original RAI-23 requested comparison of various M5 models to M5 data collected since the approval of M5. However, no COPERNIC M5 creep model comparisons to diameter change, or cladding strain, data were provided at low to moderate burnups where cladding creepdown is active. Also, cladding oxidation data were provided, but the data was not compared to the COPERNIC corrosion model used to predict M5 cladding corrosion. Provide the model comparisons to M5 cladding diameter change data at low to moderate burnups, and M5 corrosion data up to the burnups requested. Also, explain how best estimate predictions of cladding corrosion are determined based on the COPERNIC corrosion model predictions for M5.*

Response to RAI-36:

Figure 36-1: M5[®] Oxide Measurements through Figure 36-4: M5[®] Cladding Diameter Change Predictions vs. Measurements provide comparisons of COPERNIC predictions with post-irradiation examination (PIE) measurements for cladding oxide thickness and rod diameter change for AREVA NP's M5[®] database. The COPERNIC predictions agree with the measurements.

Best-estimate predictions of cladding corrosion are typically obtained using the COPERNIC fuel performance code by applying the COPERNIC best-estimate oxide model, and using the best-available data for COPERNIC inputs such as as-manufactured fuel data, best-estimate plant operating conditions, and as-operated rod power histories. No conservatism or uncertainties are used for the predictions, which are compared with PIE measurements. This differs from best-estimate cladding oxide predictions used for design calculations, which may employ bounding rod power histories and plant operating conditions, among other conservatisms.

Figure 36-1: M5[®] Oxide Measurements



Figure 36-2: M5[®] Oxide Predictions vs. Measurements



Figure 36-3: M5[®] Cladding Diameter Change Measurements



Figure 36-4: M5[®] Cladding Diameter Change Predictions vs. Measurements



RAI-37. *Is the UTL 95/95 curve in Figure 5-2 of the TR for water channel closure used in determining a penalty for DNBR as a function of burnup? If not, explain and justify why this UTL curve is not applied for determining DNBR for a given burnup.*

Response to RAI-37:

The upper tolerance limit (UTL) 95/95 curve in the topical report for water channel closure, ANP-10285P, Figure 5-2 has been used to determine the corresponding departure from nucleate boiling ratio (DNBR) penalty as a function of fuel assembly burnup based on the NRC-approved methodology defined in the topical report BAW-10147PA Revision 1 (Reference 15 in ANP-10285P). This DNBR penalty relationship has been applied to the U.S. EPR fuel assembly design.

RAI-38. *The response to RAI-25 indicates that no assembly growth data are currently available that are directly applicable to the EPR design. This is of particular concern for two reasons, the first being that there is currently a small margin to the gap between top nozzle-to-core plate, which becomes closed at end-of life, resulting in fuel assembly bowing based on the original assembly growth model. The second concern is that past experience has demonstrated that AREVA has underestimated assembly growth with M5 guide tubes. Therefore, it is possible that an NRC limitation or condition will be established on axial assembly growth until further data are provided to NRC, or design changes are implemented to substantiate that gap closure is highly unlikely at the burnup level requested.*

Response to RAI-38:

The Response to RAI-25 was not intended to indicate that fuel assembly growth data applicable to the U.S. EPR fuel assembly design does not exist. While there are no operating U.S. EPR fuel assemblies, and thus no fuel assembly growth data specifically for the U.S. EPR fuel assembly, applicable data does exist. AREVA NP acknowledges that the NRC-accepted method for defining an assembly growth model is based on empirical data for similar designs. This has historically been the case for the fuel assembly designs with zircaloy 4 guide tubes (e.g., EMF-92-116(P)(A) Revision 0). This continues to be the practice for fuel assembly designs with M5[®] guide tubes as data becomes available. For the AREVA NP fuel designs presently operating in core, empirical growth models are used to establish the maximum fuel assembly growth for calculating the available core gap margin.

The applicability of available fuel assembly growth data populations for the U.S. EPR design is based on similarities in product features and on the comparative guide tube loadings/stress ranges with the U.S. EPR design because zirconium alloy growth is largely an axial creep-induced response. Growth data for fuel assemblies with M5[®] guide tubes does exist and is applicable and sufficiently bounding for the U.S. EPR application.

The Response to RAI-25 demonstrates that the fuel assembly growth is fuel design dependent based on the guide tube loadings and stress states during the life of the fuel assembly, in addition to having a generic dependency on the material free growth response. The understanding of the comparative guide tube stress state is important in determining the relative fuel assembly growth performance and which data populations are applicable to similar fuel designs. Increased fuel assembly growth is observed for designs with higher integrated tensile stresses over the fuel assembly life compared to those with lower tensile and even compressive stresses as shown in Figure 38-1: Comparison of Calculated Average Guide Tube Stress (previously provided in RAI-25 response) and Figure 38-2: Comparison of Measured Fuel Assembly Growth. Figure 38-1 provides a comparison of average guide tube stress histories for the Mark-B12, Mark-BW, and Advanced Mark-BW lead test assembly (LTA) designs. Figure 38-2 provides the measured fuel assembly growth for these three designs and shows distinctive classes of growth behavior correlating to guide tube stress magnitudes. Use of the most bounding growth data to characterize all designs, including the U.S. EPR design, can impose an overly conservative approach that does not properly account for the inherent guide tube stress differences that drive the axial creep of the guide tubes during irradiation.

Figure RAI 38-1: Comparison of Calculated Average Guide Tube Stress



Figure 38-2: Comparison of Measured Fuel Assembly Growth



As stated in the Response to RAI-25, the primary design differences that influence the guide tube stress state are total guide tube cross section area, holddown spring preload and spring rate, and upper end grid slip load. While there are other parameters that can influence the net guide tube load, such as component pressure drop, bundle flowrate, holddown spring relaxation, grid spring relaxation, component buoyant weight, and lower shoulder gap closure, the parameters identified are the most significant for fuel assembly growth.

For the Mark-B12 and Mark-B HTP (high thermal performance) fuel assembly designs, the holddown spring preload and spring rate as well as the total guide tube cross section are the same. Differences exist primarily in the spacer grid slip loads given the different grid designs, and more specifically, in the upper end grid design. The Mark-B12 design uses an Inconel 718 upper end grid with as-designed slip loads approximately 65 percent higher than that of the Mark-B HTP zirconium alloy upper end grid. The zirconium alloy upper end grid also results in additional lower slip loads due to a faster rate of relaxation during irradiation. In addition, the as-designed bottom shoulder gap is 3 mm for the Mark-B HTP design compared to fuel rods fully seated (zero gap) for the other Mark-B designs, which results in a different loading that is less tensile.

The average guide tube stress histories for the Mark-B12 and Mark-B HTP are provided in Figure 38-3: Comparison of Calculated Average Guide Tube Stress for Mark-B12 and Mark-B HTP. The Mark-B12 design guide tube loading is shown to be much more tensile than the Mark-B HTP design. Figure 38-4: Comparison of Measured Fuel Assembly Growth, Mark-B11A/B10K/Mark-B12 and Mark-B HTP provides the measured fuel assembly growth data for the two design classes. The Mark-B12 growth data exceeds the upper fuel assembly growth design limit from BAW-10227PA, Revision 1 (Reference 7 in ANP-10285P), while the Mark-B HTP growth data is sufficiently enveloped. (Note that the measured fuel assembly growth data for the Mark-B11A and Mark-B10K designs are also included given their similarity to the Mark-B12 design.)

Figure 38-3: Comparison of Calculated Average Guide Tube Stress for Mark-B12 and Mark-B HTP



Figure 38-4: Comparison of Measured Fuel Assembly Growth, Mark-B12/B10K/B11A and Mark-B HTP



As shown in Figure 38-5: Comparison of Calculated Average Guide Tube Stress, U.S. EPR, Mark-B12 and Mark-B HTP, the U.S. EPR average guide tube stresses are enveloped by the Mark-B HTP design average guide tube stresses, which are exceeded by the Mark-B12 design average guide tube stresses for which the greatest fuel assembly growth has been measured. Therefore, the U.S. EPR fuel assembly growth is expected to be sufficiently bounded by that of the Mark-B HTP fuel assembly.

The total upper guide tube cross section for the U.S. EPR fuel assembly design is larger than that of the Mark-B12 and Mark-B HTP fuel assembly design guide tubes as shown in Table 38-1: Geometrical Comparison. The guide tube cross section is approximately 69 percent greater, which leads to a proportionately lower guide tube stress for the same loading.

The total upper end grid spacer slip load for the U.S. EPR design is approximately 31 percent lower compared to that of the Mark-B12 design, both of which are constructed with Inconel 718 material as shown in Table 38-2: Spacer Grid Spring Comparison. The lower upper end grid slip load of the U.S. EPR design coupled with the larger cross-section results in lower guide tube tensile stress.

The U.S. EPR fuel assembly upper end grid slip load is approximately 13 percent higher than that of the Mark-B HTP zirconium alloy end grid. However, the thicker guide tube for the U.S. EPR design results in lower guide tube stress than the Mark-B HTP fuel assembly design.

The holddown spring preload for the U.S. EPR design is shown in Table 38-3: Holddown Spring Parameters to be larger than the Mark-B12 and Mark-B HTP designs by 987 and 976 pounds,

respectively. By comparison, the low growth Advanced Mark-BW LTA holddown spring preload is approximately 1000 pounds greater than the respective Mark-B designs. The U.S. EPR five leaf holddown spring design also has a spring rate that is approximately four times that of the Mark-B12/Mark-B HTP holddown spring. For a given increment of growth, the corresponding increase in holddown load is proportionately greater for the U.S. EPR design. The higher preload and spring rate serves to produce lower tensile stresses and even slightly compressive stresses with burnups when compared to the Mark-B HTP, and even more so when compared to the Mark-B12 as shown in Figure 38-5. The U.S. EPR design is also shown to be better aligned with the lower growth Advanced Mark-BW LTA design as demonstrated by the guide tube stress history.

Table 38-1: Geometrical Comparison

--

Table 38-2: Spacer Grid Spring Comparison

--

Table 38-3: Holddown Spring Parameters



Given the significant difference in guide tube stresses, the use of the Mark-B12 growth data to characterize the U.S. EPR growth performance is unduly conservative. The two designs are distinctively different and should not be considered as the same class of fuel assembly design. Because of the closer aligned guide tube stress profiles, the Mark-B HTP assembly growth is expected to be applicable and bounding for the U.S. EPR design. In addition, the use of actual operating experience data accounts for the data scatter as affected by guide tube loadings and material free growth variability.

Figure 38-5: Comparison of Calculated Average Guide Tube Stress, U.S. EPR, Mark-B12 and Mark-B HTP



The U.S. EPR design limits defined in ANP-10285P, Revision 0, and the Mark-B HTP fuel assembly growth limits established from the measured data are provided in Figure 38-6: Comparison of Design Limits, U.S. EPR and Mark-B HTP. For the application of establishing empirically-based and conservative U.S. EPR fuel assembly growth design limits, the Mark-B HTP design growth limits are used, which are considered to be sufficiently bounding given the enveloping stress history of the Mark-B HTP design. The fuel assembly growth design limits affect the core plate gap, fuel rod-to-top nozzle shoulder gap and fuel assembly liftoff margins.

As reported in ANP-10285P, Revision 0, Section 5.1.7, the U.S. EPR core plate gap margin is determined using the fuel assembly growth upper design limit. The minimum fuel assembly to reactor core plate gap at end of life (EOL) for a 65 GWd/mtU maximum fuel assembly burnup was determined at worst case cold conditions for the growth limit in ANP-10285P, Revision 0. This assembly exposure exceeds what can be achieved with a limit of 62 GWd/MtU on the fuel rod. The maximum allowable U.S. EPR fuel assembly growth at cold conditions for any burnup is 0.389 percent, i.e., core gap closure based on combined tolerance of as-fabricated dimensions determined using the square root of the sum of the squares (SRSS) method. Using the fuel assembly growth upper design limit from the Mark-B HTP design shown in Figure 38-6, the U.S. EPR fuel assembly burnup is 55.7 GWd/mtU at which the predicted growth equals the maximum allowable growth of 0.389 percent. This burnup is conservative given the bounding aspect of the Mark-B HTP fuel assembly growth model relative to the U.S. EPR fuel assembly design based on a comparison of the fuel assembly design characteristics including stress state.

Figure 38-6: Comparison of Design Limits, U.S. EPR and Mark-B HTP



As reported in ANP-10285P, Revision 0, Section 5.1.7, the U.S. EPR fuel rod shoulder gap margin is determined using the fuel assembly growth lower design limit. Using the fuel assembly growth lower design limit from the Mark-B HTP design shown in Figure 38-6, the U.S. EPR minimum fuel rod shoulder gap is 1.132 inches.

As reported in ANP-10285P, Revision 0, Section 5.1.9, the U.S. EPR margin to liftoff was determined using the fuel assembly growth lower design limit and the deterministic evaluation approach. A confirmatory analysis to demonstrate adequate fuel assembly liftoff margin will be performed using the statistical holddown methodology defined in ANP-10243PA Revision 0 and approved for use in analyzing the U.S. EPR design in ANP-10263PA Revision 0. The results of this confirmatory analysis will be provided to the NRC by April 30, 2009.

The report ANP-10285P Revision 0 will be revised to include the margins for core plate gap, fuel rod shoulder gap, and fuel assembly liftoff, reported in this response when the approved version of the report is issued after receipt of the NRC safety evaluation report.

Conclusions:

1. The Mark-B HTP fuel assembly design is similar to the U.S. EPR design in guide tube stress history, and the empirically-based Mark-B HTP fuel assembly growth design limits are conservatively applicable to the U.S. EPR fuel assembly design.
2. The use of the Mark-B HTP fuel assembly growth design limits results in a maximum U.S. EPR fuel assembly burnup of 55.7 GWd/mtU, at which the maximum allowable growth of 0.389 percent at cold conditions is obtained.
3. The use of the Mark-B HTP fuel assembly growth design limits results in acceptable fuel rod-to-top nozzle shoulder gap margin (1.132 inches). The results of confirmatory analysis to demonstrate adequate fuel assembly liftoff margin will be provided to the NRC by April 30, 2009.
4. The Mark-B HTP fuel assembly growth design limits will be used for the U.S. EPR fuel assembly design until U.S. EPR data is available or until additional Mark-B HTP fuel assembly growth data alters the conservative assessment and application.
5. Additional Mark-B HTP fuel assembly growth data is scheduled to be taken at two U.S. operating plants in the fall of 2009. This data will include 1, 2, and 3 cycle operation. Growth measurements are also scheduled to be taken at two additional U.S. operating plants in January and spring 2010, which includes 2 and 3 cycle operation. In addition, growth measurements are planned for two additional plants in the spring and fall of 2010, respectively, which include 1 cycle operation. The maximum fuel assembly burnup for the assemblies to be measured is approximately 55 GWd/mtU.
6. The two concerns expressed by the NRC have been addressed:
 - Core gap margin at the most conservative condition (cold) is maintained using a conservative upper fuel assembly growth design limit that envelopes available fuel assembly growth data of a fuel assembly design that is applicable to the U.S.

EPR fuel assembly design as shown by the guide tube stress states. The core gap margins are even greater for hot operating conditions, precluding concern about fuel assembly bowing due to insufficient core gap margin.

- Considerable fuel assembly growth data for designs with M5[®] guide tubes are now available. The collection of measured data is ongoing for many different fuel assembly designs. The available data to define applicable fuel assembly growth models for fuel assemblies with similar design characteristics are sufficient and substantially more in quantity when compared to the limited amount of data used to define the upper fuel assembly design growth limits that led to the original underestimation of fuel assembly growth. The growth performance of applicable fuel assembly designs is being utilized to assess the fuel assembly growth limits for the U.S. EPR design. The design limit that is utilized bounds all of the measured fuel assembly growth data for the Mark-B HTP fuel assembly design, which has been shown to be conservatively applicable to the U.S. EPR design.

RAI-39. *Table RAI 25-1 shows that the bottom of the fuel rods are not seated as in other AREVA fuel designs. Discuss the impact of the fuel rod shifting down due to fuel assembly handling, resulting in closure of the bottom gap and the downward shift of the fuel column on fuel performance. Relating to RAI-27, did the flow tests in HERMES-P, the PETER Flow Loop, and the EOL Autoclave tests for flow induced vibration (FIV) and fretting wear account for the fact that the bottom of the fuel rods are not seated for the EPR design, thus considering no support at the bottom of the fuel rods?*

Response to RAI-39:

AREVA NP has developed multiple fuel designs using welded structures (grids welded to guide tubes) and floating structures (grids are allowed to move small distances along the guide tubes). Fuel designs using floating grids typically use seated rods. Therefore, the fuel rod's design position accompanies the grid connection condition. AREVA NP is experienced in the design and manufacture of both fuel assembly structural configurations. The high thermal performance (HTP) design is a welded structure and has always utilized lifted, or raised, fuel rods in the as-built condition.

HTP type fuel assemblies in service today are designed with the fuel rods lifted at the beginning of life. The limiting shipping and handling loads considered (at beginning of life conditions) are not sufficient to shift the fuel rods from the as-built condition. During operation, the grids are expected to relax due to irradiation, and the fuel rods are expected to seat on the lower nozzle as part of their normal and expected behavior. The timing of the fuel rods seating varies versus as-built height, fuel rod burnup, and grid slipload retention forces. In general, the seating of the fuel rods in an HTP design occurs at the end of the first cycle or early second cycle of operation for 18-month cycles, and typically after the first cycle for 24 month cycles. The downward shift of the fuel column is expected and this design attribute is represented in the current HTP fuel operating experience. Fuel rod growth is not impacted by the lifted condition. The performance impact of the lifted fuel rod is largely limited to partially decoupling the fuel rod growth from the fuel assembly skeleton by reducing the influence of fuel rod growth on the guide tube stress. AREVA NP HTP fuel designs (with fuel rods raised in the as-built condition) are currently operating successfully in the U.S. in CE 14x14, CE 15x15, B&W 15x15, Westinghouse 15x15, and Westinghouse 17x17 plants.

ANP-10285P, "U.S. EPR Fuel Assembly Mechanical Design Topical Report," Section 5.1.4 justifies the U.S. EPR HTP design's resistance to fretting based on multiple out-of-pile performance tests. These tests demonstrate acceptable performance under extreme operating conditions. The fuel assembly testing performed in the HERMES-P loop was configured with the fuel rods in a lifted condition, reflecting the as-designed condition.

The PETER Flow Loop tests were designed to quantify the vibration response of the fuel rods and fuel assembly versus flow rate. The fuel assembly was tested with fuel rods in lifted condition to assess the fuel rod vibration response.

The end of life (EOL) autoclave tests are single rod tests performed using only three grid segments (lower end grid segment and two intermediate grid segments). Therefore, no bottom support of the fuel rod was present.

Therefore, the flow tests in HERMES-P, the PETER Flow Loop, and the EOL Autoclave tests for flow induced vibration (FIV) and fretting wear account for the fact that the bottom of the fuel rods are not seated for the U.S. EPR design.

RAI-40. *The strain data provided in Table RAI 28-1 is not applicable to the one percent elastic plus uniform plastic strain limit in the SRP, or the EPR design limit that is meant to prevent brittle failure in fuel cladding. The strain data provided in RAI-28 is based on total elongation data that includes total plastic strain, and not uniform plastic strain as required by the SRP limit. Cladding failure due to brittle fracture has been observed in Garde et al. (1996) and Hermann et al. (2007) with measured total plastic elongations between 1 to 3.6 percent from seven separate specimens, including three axial tensile and four burst test specimens. These specimens failed in a brittle manner with failure below the yield strength, at 60 to 85 percent of yield strength. Therefore, the plastic strain should be near zero, suggesting that maintaining total plastic elongation above one percent will not prevent brittle behavior. The measured uniform plastic strains from the tests in Garde et al. (1996) and Hermann et al. (2007) were less than 0.5 percent. Provide irradiated M5 strain data in terms of either elastic plus uniform plastic strain, or uniform plastic strain, confirming that the EPR one percent elastic plus uniform plastic limit is met at the maximum fluence and hydrogen level expected for the EPR fuel design.*

Referenced papers:

A. M. Garde et al., "Effects of Hydride Precipitate Localization and Neutron Fluence on the Ductility of Irradiated Zircaloy-4," *Zirconium in the Nuclear Industry: 11th International Symposium, ASTM STP 1295*, p. 407, American Society for Testing and Materials, Garmisch-Partenkirchen, Germany (1996).

A. Hermann, S. K. Yagnik, and D. Gavillet, *Effect of Local Hydride Accumulations on Zircaloy Cladding Mechanical Properties, 15th International Symposium on Zirconium in the Nuclear Industry, American Society for Testing Materials, Sun River, Oregon (2007).*

Response to RAI-40:

Uniform elongation (elastic plus uniform plastic) data for irradiated Alloy M5[®] fuel rod cladding at room and elevated temperature is presented in Table 40-1: M5[®] Uniform Elongation. This elastic plus uniform plastic data derives from axial tensile tests performed at 20°, 25°, and 350°C on M5[®] fuel rod cladding irradiated in a pressurized water reactor (PWR). The data in Table 40-1 presents the uniform elongation value versus temperature, burnup, and fluence. Table 40-1 demonstrates that the 1 percent strain limit is applicable to M5[®] cladding.

The hydrogen content of the M5[®] cladding tested was "typical" for the burnup (fluence) achieved. This means that it was in the range shown in Figure 40-1: M5[®] Hydrogen Content. From this plot of hydrogen content versus burnup, it is evident that the hydrogen content for M5[®] fuel rod cladding is much less than that of Zr-4 (and other zirconium alloys) at high burnup. At the current licensed burnup of 62,000 MWd/tU, the hydrogen content of Zr-4 cladding is approaching 700 ppm, while in alloy M5[®], it is less than 100 ppm. The accompanying photomicrograph shows circumferential hydride in M5[®] cladding irradiated to 70,000 MWd/tU and having total hydrogen content of 70 ppm. This is the typical and expected hydrogen performance of alloy M5[®] irradiated in a PWR.

The data also shows that the evolution of hydrogen with burnup for alloy M5[®] is approximately linear and that the majority of the hydrogen content is reached at relatively low burnup.

This response demonstrates that alloy M5[®] cladding has been tested under tensile conditions at end of life burnups with hydrogen content typical for the alloy and that the 1 percent strain criterion is applicable to M5[®] cladding. Thus, the 1 percent strain limit is applicable to M5[®] cladding at the current licensed PWR burnup limit and at potentially higher future burnups.

Table 40-1: M5[®] Uniform Elongation

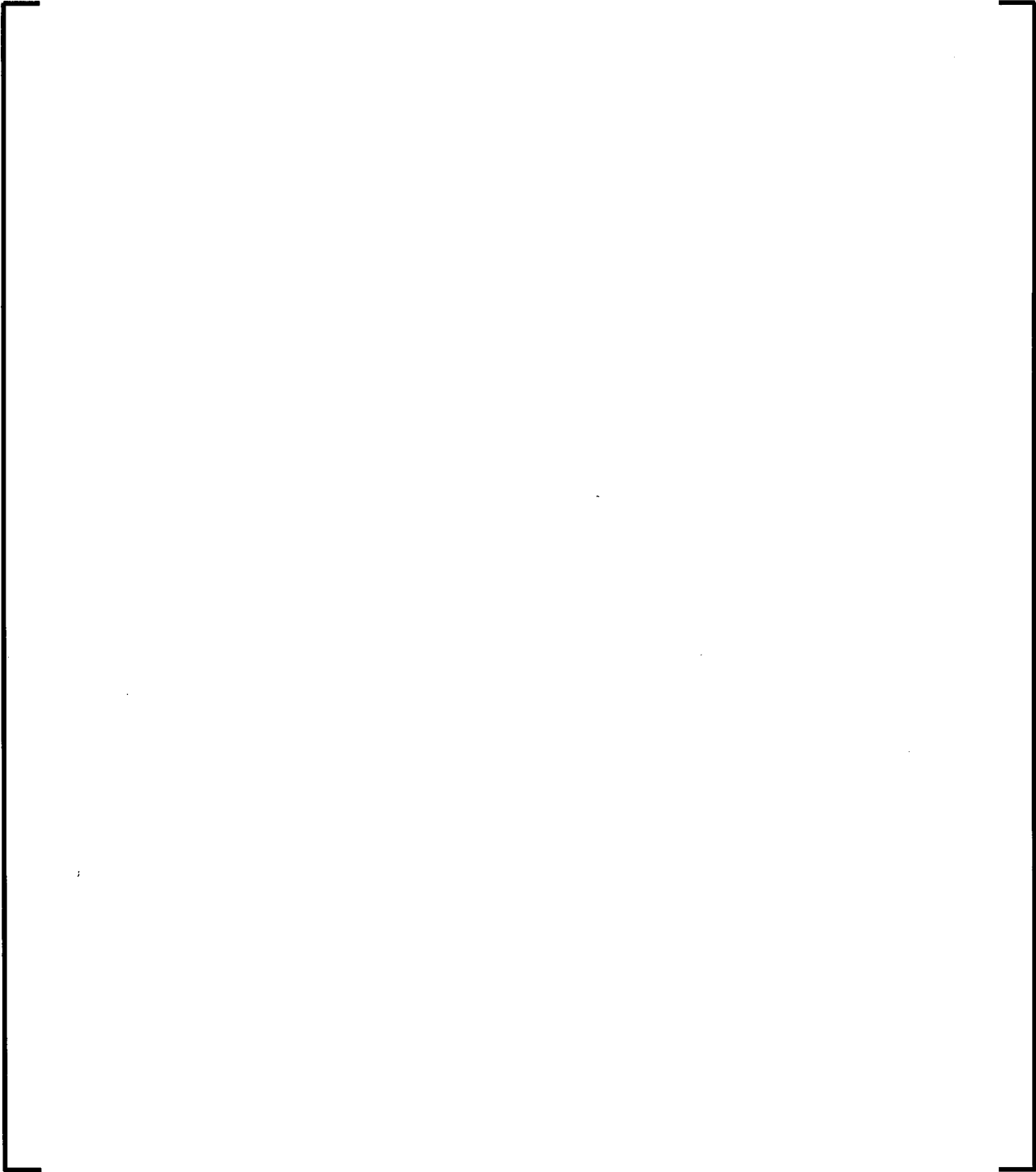
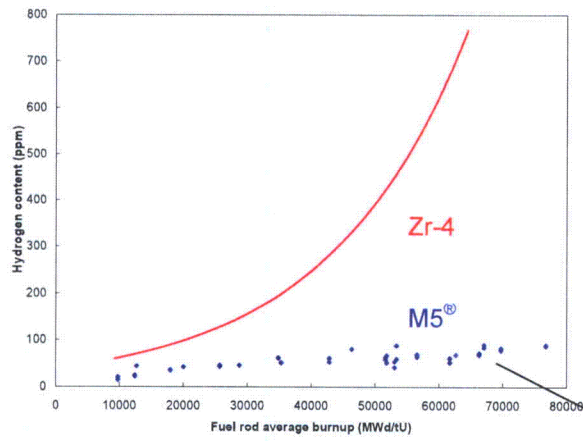
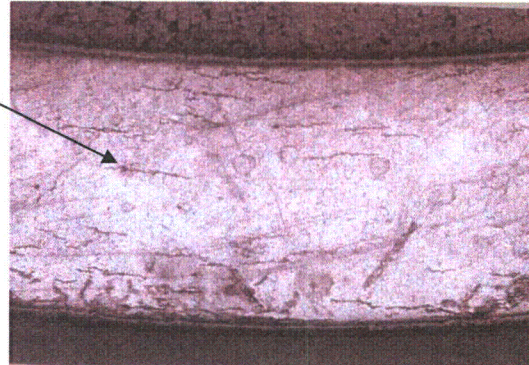


Figure 40-1: M5[®] Hydrogen Content



*70 ppm Hydrogen
at 70,000 MWd/tU*



RAI-41. *Some of the design input conditions between the COPERNIC and RODEX2-2A codes for SBLOCA analyses, and the RODEX3A code for RLBLOCA analyses are not the same for the EPR fuel design analyses. The design input conditions in question include rod pressure, cladding strain, and fuel melt analyses. For example, the input initial rod pressure for COPERNIC and RODEX2-2A was 304.7 psi while for the RODEX-3A analysis it was 290 psi. The rod densification for COPERNIC was 1.5 percent TD while for RODEX2-2A and RODEX3A was 2.0 percent TD. Also, the enrichment for RODEX2-2A was only 3 percent while for COPERNIC and RODEX3A it was 4.8 and 4.95 percent, respectively. Explain why these differences exist.*

Response to RAI-41:

The differences noted in the question are related to the different uses of COPERNIC and the RODEX codes. COPERNIC is used for non-loss of coolant accident (LOCA) applications and various aspects of fuel design, including rod internal gas pressure, fuel melting, and clad strain. The RODEX codes are limited to LOCA applications. While enrichment plays a minor role in LOCA analysis, it does affect the burnup dependent pellet radial power profile. Each enrichment fuel rod type from the neutronics design calculations were evaluated using COPERNIC. For the amount of densification modeled, RODEX LOCA analyses use a conservatively high upper tolerance value. COPERNIC non-LOCA analyses use a nominal value within the fuel specifications for the calculations, including a bias towards the lower tolerance resintering value for the uncertainty treatment in the internal pressure calculations.

Enrichment

RODEX2-2A and RODEX3A use different enrichments because of different computational processes. For the limiting realistic large break loss of coolant accident (RLBLOCA) case, RODEX3A uses an enrichment of 4.95 weight percent. That enrichment is taken from the neutronics generated power history files for the peak $F_{\Delta H}$ UO₂ rod at the sampled time in cycle by the RLBLOCA automation process. Thus, the enrichment changes depending on which fuel rod has the peak $F_{\Delta H}$ at the sampled time in the cycle.

RODEX2-2A uses a fixed three weight percent enrichment taken as the RODEX2-2A default for the small break loss of coolant accident (SBLOCA) analysis. This choice is conservative and leads to higher initial fuel temperatures (stored energy). A calculation was performed to estimate the magnitude of the fuel temperature reduction for the SBLOCA initialization when the enrichment is increased from 3.0 to 4.95 weight percent. The calculation is identical to that of the SBLOCA steady state initialization except for the increase in enrichment. Table RAI 41-1: Pellet Volume Average Temperatures at Two U235 Enrichments shows the volume averaged fuel temperatures for the two enrichments and for the four fuel rod types in the SBLOCA model. The axial maximum volume average temperature change for the hot rod is -22.6°F. Thus, the original SBLOCA computation using 3.0 weight percent enrichment has higher initial stored energy than if a more realistic enrichment had been used.

Pellet Resinter Densification

The pellet resinter densification of 2.0 percent of theoretical density (%TD) is a maximum upper limit from fuel manufacturing specifications and it is used in both RODEX2-2A and RODEX3A. The pellet resinter densification used in COPERNIC calculations is a nominal value. The values reported in ANP-10285P, Table 3-8 and Table 3-9 are incorrect. The maximum resinter

densification in topical report ANP-10285P, Table 3-8 and Table 3-9 will be changed to the fuel manufacturing specification, []. The Resinter Densification Limits for the UO₂ and Gadolinia fuel pellet parameter tables will be changed as follows in the NRC-approved version of the topical report:

Table 3-8 UO₂ Pellet Parameters

Change [] to []

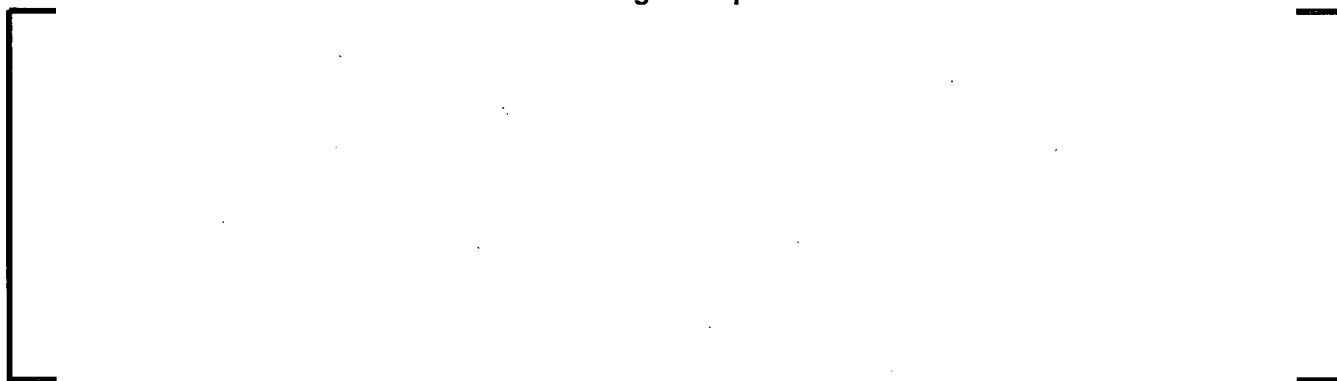
Table 3-9 Gadolinia Pellet Parameters

Change [] to []

Internal Pressure

The internal pressure discrepancy is concerned with the units. The pressures are 304.7 psia versus 290 psig; thus, the absolute pressures are the same.

Table RAI 41-1: Pellet Volume Average Temperatures at Two U235 Enrichments



RAI-42. *Due to the extremely small margin for the shipping loads for bottom and top nozzles, further details of these calculations are necessary. Provide the details, including any assumed conservatisms, of both the analyses, including mesh sizes and structure of the mesh assumed if FEA was used for these calculations.*

Response to RAI-42:

A finite element analysis (FEA) was performed for both the top and bottom nozzles for the shipping and handling load evaluation.

To show compliance with specific loadings and resulting margins, the general approach is to use as conservative and simplistic an approach as possible. Since the ASME Code has built-in margins, the goal is to use appropriate FEA models, as long as the resulting margins are positive. In other words, if a margin of 1.01 percent is shown, it is concluded that the criterion has been met and additional analyses are not performed to demonstrate a greater margin.

Top Nozzle:

The top nozzle analysis was performed with an ANSYS FEA model. Several conservatisms were used in the analysis:

- a. The model used a uniform loading, taking the full 4g shipping load and distributing it in a uniform pattern at each guide tube location. The load will try to follow the stiffest load path. Because the center of the plate deflects, higher loadings will be experienced at the guide tube locations closer to the edge of the nozzle, an effect termed mal-distribution. Therefore, if mal-distribution is taken into account, higher loads would be experienced at the edges and lower loads towards the center. As a result, the net deflection of the center of the nozzle would be less. The membrane plus bending stresses for the nozzle would be lower, and the resulting margins higher.
- b. An actual 4-g shipping load is a short duration, dynamic impact loading. The loads applied in the model are static loads. No provision was made to account for any increase of the material strength from dynamic loadings (i.e., an increase in material strength due to strain rate effects).
- c. The supports for the grids, inside the shipping container, would provide some restraint to the axial motion of the fuel assemblies. However, the analysis assumes that the full 4-g load is being applied to the nozzle.
- d. The complete fuel assembly weight was taken to bear on the top nozzle. Simply reducing the total weight by the weight of the nozzle itself, and calculating a slightly lower 4-g loading produces an increase in the margin of safety (MS) from []].

Model Mesh Sizing:

The mesh sizing used for the top nozzle was similar to the meshing used for like nozzles in past analyses. The actual U.S. EPR top nozzle FEA model used a total of 131,619 nodes and 92,096 elements. Previous studies on similar nozzles have shown that this is adequate to

represent not only membrane and membrane plus bending, but also peak stresses. The previous study indicated that the number of elements should be at least 80,000.

The ideal aspect ratio for finite elements is a 1:1 ratio. Ratios as high as 5:1 are acceptable. The typical ratio of the brick elements in the top nozzle FEA model in the region of highest stresses was approximately 3.3:1.

Bottom Nozzle:

While the grillage of the top nozzle is made from machining a solid plate, the bottom nozzle is made up of thin curved plates, interconnected by a series of upper and lower rods being brazed into the curved plates and into the side walls of the nozzle.

Due to the complexity of the lower nozzle, the FEA model was used in a lower bound collapse load approach, as permitted by the ASME Code.

The following conservatisms were used for the bottom nozzle analysis:

- a. The model used a uniform loading, taking the full 4-g shipping load and distributing this load in a uniform pattern at each guide tube location. This was similar to the top nozzle loading.
- b. As with the top nozzle analysis, no provision was made to account for any increase of the material strength due to dynamic loadings.
- c. As with the top nozzle analysis, no provision was made to reduce the loading on the bottom nozzle due to the axial restraint provided at the grid supports.
- d. The complete fuel assembly weight was taken to bear on the bottom nozzle. The total load could have been reduced by simply reducing the total weight by the weight of the nozzle itself, and calculating a slightly lower 4-g loading.
- e. In determining the lower bound collapse load, an elastic-plastic material stress strain curve was used, using the criteria identified in ASME Code, Appendix F, Article F-1000. While the code allows the use of 2.3 Sm (1.533 Sy) as the criterion, a lower value of 1.0 Sy was used instead. The elimination of this conservatism would provide an increase in the margin.

Actual test data for the bottom nozzle showed that a loading of more than three times the collapse load of the model was obtained, without a full collapse of the nozzle. The results of the test data could have been used in the calculation of the margin of safety, but because the FEA model did show a positive margin, the FEA model results were used.

Further, because the actual test data demonstrated that the FEA model was conservative, there was no attempt to perform a mesh breakup study for the bottom nozzle model. The vertical vanes were broken up into six elements through the height, with aspect ratios approaching a 1:1 ratio.

For the normal operating and the faulted conditions, the test data for the bottom nozzle was used and not the FEA model.

RAI-43. *The strain limit on the guide tube end plug appears to be related to the unirradiated condition that is applicable to reactor startup of a fresh fuel assembly, but the strain limit is significantly less following irradiation. What is the plastic strain experienced during subsequent startups of this assembly after being irradiated?*

Response to RAI-43:

There is no additional plastic strain experienced by the guide tube end plug during subsequent startups. The plastic strain induced during the initial startup for a fresh assembly is based on the temperature and the difference in thermal expansion coefficients between the end plug and the bolt. During subsequent startups, the same temperature and the same total strain is reached, and no additional plastic strain is incurred. Therefore, unirradiated material properties for the guide tube lower end plug are appropriate.

RAI-44. *PNNL has performed a cladding strain analysis with the FRAPCON-3.3 code using the input provided for the COPERNIC strain analysis. The results of the FRAPCON-3 analysis has demonstrated that at a burnup of 28.5 GWd/MTU a 3.3 kW/ft lower cladding strain limit, and at a burnup of 53.5 GWd/MTU a 1.9 kW/ft lower limit for the UO₂ EPR fuel rods than calculated by COPERNIC in Table RAI 22-4. For the UO₂-Gd₂O₃ EPR fuel rods the LHGR limit calculated by FRAPCON-3 was approximately 2 kW/ft lower at 32.7 GWd/MTU and only 0.2 kW/ft lower at 52.9 GWd/MTU than calculated by COPERNIC in Table RAI 22-6.*

- a. *Provide the values of the LHGR limits used for AOOs for the EPR design above burnups of 26 GWd/MTU for the UO₂ and UO₂-Gd₂O₃ EPR fuel rods, respectively, if they are different from the COPERNIC LHGR values in Tables RAI 22-4 and 22-6. Do these values include the uncertainty in COPERNIC predictions of cladding strain based on the strain predictions?*
- b. *If these values do not include uncertainties in COPERNIC strain predictions, justify the lack of including predictive uncertainties in COPERNIC based on the general under-predictions demonstrated in Figure 7-44 of BAW-10231P of the TRANSRAMP IV ramp data.*

Response to RAI-44:

- a. The linear heat generation rate (LHGR) limit values given in the Response to RAI-22 were for a specific UO₂ and eight w/o gadolinia fuel rod in the 18-month equilibrium cycle using the power history information provided in the Response to RAI-21 and RAI-22 tables. The results are specific for those rods as a function of burnup and are best-estimate values calculated with the methods described in BAW-10231. The limits for each fuel rod type are provided in topical report ANP-10285P, Figure 5-8. These curves are generated by taking a composite enveloping minimum LHGR for each fuel rod type from the set of depletions performed for the transition from Cycle 1 to equilibrium for both the 18-month and 24-month cycles. For the LHGR limits used for the anticipated operational occurrence (AOO) safety analysis for the U.S. EPR design, a single minimum LHGR limit value for each fuel type was chosen on the basis of the maximum rod exposure in the limiting fuel assemblies. This limit value is specified for a maximum fuel rod exposure in the fuel assembly that would have the limiting power during normal operation and AOOs. The limiting rod exposure was also determined for each of the cycles of operation, and the maximum burnup was conservatively selected to provide the lowest LHGR limit. This exposure is typically near the end of the first operational cycle of the fuel assembly and takes credit for the fact that fuel assemblies with burnups higher than this level are not limiting with respect to LHGR. These values are adjusted based on the peak power capability of the gadolinia fuel rods as compared to the peak UO₂ fuel rod. The value used was [], which is derived for this analysis from the four w/o gadolinia fuel rod.
- b. [] (setpoints analysis). The methods employed to protect the fuel centerline melt (FCM) and one percent clad strain to a 95/95 confidence level are outlined in the ANP-10287P topical report. The setpoints incorporate uncertainties []

J. For the U.S. EPR FSAR Tier 2, Chapter 15 accident analysis, the nominal setpoint for the high linear power density (HLPD) reactor trip (RT) was 14.0 kW/ft (460 W/cm) (refer to U.S. EPR FSAR Tier 2, Table 15.0-7—Reactor Trip Setpoints and Delays Used in the Accident Analysis). In addition, the incore monitoring system protects the fuel rods from experiencing departure from nucleate boiling ratio (DNBR), which can provide further margin to the limiting LGHR required to reach FCM and/or one percent clad strain.

As discussed in the COPERNIC SER (BAW-10231PA Revision 1), COPERNIC generally provides accurate or conservative predictions of cladding strain versus the available data. As described in Section 7.2.2.3.3 of the COPERNIC topical report, BAW-10231PA Revision 1, [

J.

RAI-45: *The RODEX3A model has been used to determine fuel center line temperature, gap conductance and fuel thermal conductivity in support of EPR LBLOCA. The staff is concerned that the RODEX3A code and the procedures described on Page 4-93 of EMF-2103 revision 0 may lead to underestimating the fuel centerline temperature. Provide appropriate responses to the following questions.*

- a. *Is the fuel temperature database for the correlation used by AREVA for RODEX3A applicable to EPR fuel and most current fuel designs? If yes, provide an explanation of the database's applicability to the U.S. EPR design.*
- b. *Is the expanded RODEX4 database for fuel temperatures more applicable to EPR fuel design? If so, has it been used to verify the RODEX3A results? Provide comparisons of these data in terms of the ratio of predicted-minus-measured divided by measured temperature and also the predicted-minus-measured temperature.*
- c. *The RODEX4 code treats the fuel conductivity in different fuel regions, for example the rim and bulk regions, while the RODEX3A code does not. Discuss the impact of this difference in integral thermal conductivity between the two codes on initial stored energy.*

EMF-2103 revision 0, "Realistic Large break LOCA for Pressurized Water Reactors." August 2001.

Response to RAI-45:

The issues in this question coincide with the concern expressed by the NRC that the RODEX3A code and the offset correlation used to correct for RODEX3A temperature underprediction might be underestimating centerline temperature.

The RODEX3A temperature calculation issues can be summarized as follows:

- RODEX3A is not fully accounting for burnup degradation of fuel thermal conductivity, which results in a burnup-dependent, underpredicting bias.
- This underpredicting bias is corrected in applications by adjusting the RODEX3A calculated temperatures by the bias offset correlation.

The responses to the three parts of RAI-45 are provided.

- a. The fuel temperature database used to benchmark RODEX3A is applicable to the U.S. EPR and current pressurized water reactor (PWR) fuel designs. The NRC approval for the use of RODEX3A in realistic large break loss of coolant accident (RLBLOCA) analyses specifically encompasses Westinghouse (3 and 4 loop plant types) and Combustion Engineering plant types. The fuel assembly design for the U.S. EPR is (with respect to issue affecting the fuel performance code) identical to current PWR fuel assembly designs. RODEX3A is applicable to the U.S. EPR fuel design assembly because:

- The fuel material is the same, namely UO_2 , and the fuel thermal conductivity is a material property and not design- or reactor-type specific.
- The temperature database verifies both fuel thermal conductivity when the gap is closed or almost closed and the heat transfer in the gap when the gap is open. Both conditions are needed to determine the bias and uncertainty scatter for application.

The temperature database characteristics bound those of the fuel rods used in current operating reactors and the U.S. EPR rather than matching exactly. This is a desirable characteristic because the details of the fuel rod can evolve over time.

- b. The temperature database used for the code RODEX4 is applicable to current operating plants and the U.S. EPR. This applicability is explained in Part a. The temperature database for RODEX4 contains the data used to benchmark RODEX3A, additional data with similar characteristics to the data in the RODEX3A database, and data beyond the 30 MWd/kgU used in the RODEX3A database up to about 100 MWd/kgU. Therefore, it is appropriate to benchmark RODEX3A on the extended RODEX4 database. The results are presented in Figure RAI 45-1: Comparison of RODEX3A Temperature Correlation to an Expanded Database - Linear Fit and Figure 45-2: Comparison of RODEX3A Temperature Correlation to an Expanded Database - Quadratic Fit.

Figure 45-1 presents a comparison of the existing RODEX3A fit to the original database against the expanded database. The RODEX3A current fit is conservative when compared to the expanded RODEX4 database because it is below a revised fit to the expanded database.

The RODEX3A calculations of the expanded database are not fit well with a linear correlation. Figure 45-2 shows that a quadratic fit represents the RODEX3A predictions of the expanded database more accurately. The current linear fit is below the parabolic fit, which reinforces the conclusion that the current linear fit is conservative. Figure 45-3: Comparison of RODEX3A Temperature Predictions to an Expanded Data Base – Relative Differences presents the comparison in terms of a relative difference (as requested in the question), i.e., $(T_{\text{calc}} - T_{\text{meas}}) / T_{\text{meas}}$.

The uncertainty scatter is smaller for both the linear and the quadratic fits, in terms of overall the extended database, as well as when limited to the 0 to 30 MWd/kgU interval. In the linear fit, the standard deviation for the entire extended database is 110.3°F, while for the 0 to 30 MWd/kgU interval, the standard deviation is 127°F, both of which are smaller than the current value of 130°F.

In the December 2008 NRC audit in Rockville, MD, on RODEX3A, the NRC reviewers commented that two cases in the original database, namely IFA-432 Rods 2 and 6, are not representative of current fuel designs and might bias the statistics of the temperature benchmarking. These cases are also in the expanded database used for RODEX4.

One of the two fuel rods has a very large initial gap and the other has a very low pellet initial density, both of which are outside the current design specifications. This is consistent with the cases in the benchmark data set because the characteristics of current fuel designs are bounded rather than matched. The characteristics of these two

cases are very bounding. It is legitimate (and desirable when possible) to validate the code for a wider range of characteristics than expected in the actual application.

However, in order to address the concern regarding those two fuel rods of the Halden database, the comparison was performed without the two cases. Very small changes were noticed in the linear and quadratic fits, but the conclusion that the existing linear fit is conservative is still supported, as illustrated in the Figure 45-4: Comparison of RODEX3A Temperature Correlation to an Expanded Data Base, but Without IFA-432 Rods 2 and 6 – Quadratic Fit. The standard deviation is improved by a few degrees.

Figure 45-1: Comparison of RODEX3A Temperature Correlation to an Expanded Data Base - Linear Fit



Figure 45-2: Comparison of RODEX3A Temperature Correlation to an Expanded Data Base - Quadratic Fit



Figure 45-3: Comparison of RODEX3A Temperature Predictions to an Expanded Data Base – Relative Differences



Figure 45-4: Comparison of RODEX3A Temperature Correlation to an Expanded Data Base, but Without IFA-432 Rods 2 and 6 – Quadratic Fit



- c. The code RODEX3A does not treat the rim of the fuel pellet differently than the interior region like RODEX4 does. A high burnup structure forms at the outer pellet rim at local burnups greater than about 63 MWd/kgU (which corresponds to a pellet average burnup greater than 45 to 50 MWd/kgU, depending on specific radial power profile).

The rim formation involves a recrystallization process where new, small grains are formed and the fission products are swept to grain boundaries and into the new large pores that also formed. This restores the matrix thermal conductivity mitigating the burnup degradation effects. However, the large pores formed in the rim are degrading the thermal conductivity. RODEX3A does not model the high burnup structure in the rim region as RODEX4 does.

RODEX3A overestimates the temperature jump in the pellet-to-cladding gap because its model conservatively underestimates the gap heat transfer coefficient.

For this reason, a temperature overprediction occurs at the beginning of life, between 0 and 10 MWd/kgU. The underestimate of the centerline temperature due to the

incomplete accounting for the burnup degradation of thermal conductivity is compensated by the overestimate of the gap temperature jump up to a burnup of about 10 MWd/kgU, after which the lack of modeling the burnup degradation of thermal conductivity becomes dominant (this issue is addressed by the offset bias correction).

While the code RODEX3A does not have as detailed a model for the effects of burnup on the pellet thermal conductivity, the use of a bias offset based on a fit of the RODEX3A predictions to the measured data compensates for this.